

AD-A131 153

TECHNICAL
LIBRARY

AD#-131153

TECHNICAL REPORT ARBRL-TR-02502

A LABORATORY ARC DRIVEN RAIL GUN

Keith A. Jamison
Henry S. Burden

June 1983



US ARMY ARMAMENT RESEARCH AND DEVELOPMENT COMMAND
BALLISTIC RESEARCH LABORATORY
ABERDEEN PROVING GROUND, MARYLAND

Approved for public release; distribution unlimited.

Destroy this report when it is no longer needed.
Do not return it to the originator.

Additional copies of this report may be obtained
from the National Technical Information Service,
U. S. Department of Commerce, Springfield, Virginia
22161.

The findings in this report are not to be construed as
an official Department of the Army position, unless
so designated by other authorized documents.

*The use of trade names or manufacturers' names in this report
does not constitute indorsement of any commercial product.*

REPORT DOCUMENTATION PAGE		READ INSTRUCTIONS BEFORE COMPLETING FORM
1. REPORT NUMBER TECHNICAL REPORT ARBRL-TR-02502	2. GOVT ACCESSION NO.	3. RECIPIENT'S CATALOG NUMBER
4. TITLE (and Subtitle) A LABORATORY ARC DRIVEN RAIL GUN		5. TYPE OF REPORT & PERIOD COVERED Technical Report
		6. PERFORMING ORG. REPORT NUMBER
7. AUTHOR(s) Dr. K.A. Jamison and Mr. Henry S. Burden		8. CONTRACT OR GRANT NUMBER(s)
9. PERFORMING ORGANIZATION NAME AND ADDRESS US Army Ballistic Research Laboratory ATTN: DRDAR-BLB Aberdeen Proving Ground, MD		10. PROGRAM ELEMENT, PROJECT, TASK AREA & WORK UNIT NUMBERS DA Project 1L16112603AH18
11. CONTROLLING OFFICE NAME AND ADDRESS US Army Armament Research & Development Command US Army Ballistic Research Laboratory (DRDAR-BLA-S) Aberdeen Proving Ground, MD 21005		12. REPORT DATE June 1983
		13. NUMBER OF PAGES 52
14. MONITORING AGENCY NAME & ADDRESS (if different from Controlling Office)		15. SECURITY CLASS. (of this report) UNCLASSIFIED
		15a. DECLASSIFICATION/DOWNGRADING SCHEDULE
16. DISTRIBUTION STATEMENT (of this Report) Approved for public release; distribution unlimited.		
17. DISTRIBUTION STATEMENT (of the abstract entered in Block 20, if different from Report)		
18. SUPPLEMENTARY NOTES		
19. KEY WORDS (Continue on reverse side if necessary and identify by block number)		
Rail gun Macroparticle Launcher Opening Switch Railgun Mass Accelerator Plasma Arc Driven Mass Driver Propulsion Armature Dynamics Electromagnetic EM-Driver Arc Armature EM-Guns Exploding Wire		
20. ABSTRACT (Continue on reverse side if necessary and identify by block number) (idk) A laboratory, single stage, arc driven rail gun and its associated power supply have been designed, constructed and operated. Diagnostic probes have been fabricated to assess the performance of the rail gun and power circuit. The operation and performance of this system will be described in this report.		

TABLE OF CONTENTS

	<u>Page</u>
LIST OF ILLUSTRATIONS	5
LIST OF TABLES	7
I. INTRODUCTION	9
II. POWER CIRCUIT	10
A. Capacitor Bank	12
B. Storage Coil	14
C. Closing Switch	14
D. Opening Switch	14
E. Arc Initiator	17
F. Connections	19
III. RAIL GUN	19
A. Design Features	19
B. Projectiles	21
IV. MEASUREMENT DEVICES	21
A. Fast Rogowskii Coil	22
B. Voltage Divider	22
C. Slow Rogowskii Coil	23
D. Ballistic Pendulum	23
V. PERFORMANCE	23
A. Breech Voltage	24
B. Capacitor Discharge Current	27
C. Arc Current	29
D. Velocity	30
VI. CONCLUSION	32
ACKNOWLEDGEMENTS	32
REFERENCES	33
APPENDIX A - EXPLODING WIRE OPENING SWITCH CALCULATIONS	35
APPENDIX B - RAIL GUN PERFORMANCE	45
DISTRIBUTION LIST	49

LIST OF ILLUSTRATIONS

<u>Figure</u>		<u>Page</u>
1	Rail Gun Schematic	11
2	Intermediate Inductive Storage Circuit	13
3	Trigatron Closing Switch	15
4	Exploding Wire Opening Switch	16
5	Arc Armature Initiator	18
6	Cross Section View of Barrel Assembly	20
7	Location of Measurement Probes	25
8	Breech Voltage Versus Time	26
9	Capacitor Discharge Current Versus Time	28
10	Arc Current Versus Time	31
A1	Calculated Capacitor Current	38
A2	Exploding Wire Performance Versus Wire Gauge	40

LIST OF TABLES

Table	Page
1. Flux Change Conditions	29
B1. Summary of Rail Gun Performance	47

I. INTRODUCTION

Electromagnetic propulsion of projectiles is militarily attractive as an alternative to chemical propellants for a variety of reasons. It is not subject to velocity limits inherent in propulsion by expansion of gases. Also, its energy may be derived from widely available and relatively inert diesel fuel, thus obviating some logistic and safety problems associated with chemical propellants. Laboratory electromagnetic mass accelerators have produced velocities up to 10 km/s ,¹ which is far in excess of the velocity available by conventional propulsion. The increased muzzle velocity promises greater hit probability and improved lethality.

The concept of electromagnetic propulsion has existed for more than 60 years;² experimental devices of various performance levels have been built since the 1940's.³⁻⁷ The simplest and most studied device is the rail gun (to be described below) but other configurations with stationary coils driving moving inductors are also popular. Among rail guns, there are both solid armature and plasma arc armature types. Experimental studies have shown that the plasma arc armature driver has a very low mass and promises good sliding electrical contact with immunity to high pressure and acceleration. Several successful laboratory arc armature rail guns have demonstrated these attributes to varying degrees. Although attractive, the arc armature has not been extensively studied experimentally. This has prompted us to build a diagnostic arc armature mass accelerator for experimental testing of the prediction of existing arc dynamics theory.⁸ Our rail gun has been designed and constructed as a

¹R.S. Hawke, A.L. Brooks, F.J. Deadrick, J.K. Scudder, C.M. Fowler, R.S. Caird and D.R. Peterson, "Results of Rail Gun Experiments Powered by Magnetic Flux Compression Generators," *IEEE Trans. on Magnetics*, Mag. 18, 82 (1982).

²A.L.O. Fauchon-Villeplee, *Electric Cannons*, 1921. Also see US Patent Nos. 1,370,200 patented 1 Mar 21, 1,421,435 patented 4 Jul 22 and 1,422,427 patented 11 Jul 22.

³Summary of work done by J. Hänsler, "Electric Gun and Power Source," *Armour Research Foundation Report No. 3 on Project No. 15-391-E* (1946).

⁴D.E. Brast and D.R. Sawle, "Study of Rail-Type MHD Hypervelocity Projectile Accelerator," *Proceedings of the Seventh Hypervelocity Impact Symposium*, Vol. 1, 187 (1964).

⁵J.P. Barber, "The Acceleration of Macroparticles and a Hypervelocity Electromagnetic Accelerator," *Ph.D. Thesis*, Australian National University, Canberra, Australia (1972).

⁶S.C. Rashleigh and R.A. Marshall, "Electromagnetic Accelerator of Macroparticles to High Velocities," *J. Appl. Phys.* 49, 2540 (1978).

⁷N.H. Wrobel and M.J. Newman, "System Study to Determine Future K E Propulsion Conventional/Electric Gun or Rocket/Ramjet?" *Proc. 6th Int. Symp. on Ballistics* (1981), p. 546.

⁸J.D. Powell and J.H. Batteh, "Plasma Dynamics of an Arc-Driven, Electromagnetic, Projectile Accelerator," *J. Appl. Phys.* 52, 2717 (1980); "Two-Dimensional Plasma Model for Arc-Driven Rail Gun," *J. Appl. Phys.* (in press).

tool to improve the understanding of high pressure, high temperature, driven arc dynamics and to find the ideal armature for the driver of a rail gun.

The principal components of a rail gun are shown schematically in Figure 1. The power supply drives the current I down the upper rail, across a plasma arc armature from rail to rail, and back through the lower rail. The right-hand rule predicts an inward pointing magnetic field between the rails for both forward current in the upper rail and the returning current in the lower rail. The accelerating Lorentz force is produced by the interaction $\vec{I} \times \vec{B}$ between the current in the armature and the field B created about the rails. Its direction is that of the cross product; its magnitude for the rail gun configuration may be written in the form

$$F = \frac{1}{2} \frac{dL_r}{dx} I^2, \quad (1)$$

which is simply the derivative of the energy associated with the rail inductance with respect to the direction of motion of the armature; $\frac{dL_r}{dx}$ is the inductance per unit length of the rail pair.

Practical restrictions on the magnitude of the current are imposed by peak forces. To utilize the entire length of the rails the current must be supplied to the rails for a time sufficient to bring the accelerating projectile up to speed within the length of the barrel. Tradeoffs between available storage capacitors, theoretical efficiency, circuit losses, projectile masses, desired velocities, pressure tolerances, and switch performance lead to the following experimental characteristics:

- o Current $\sim 10^5$ amperes
- o Current pulse duration $\sim 2 \times 10^{-3}$ s ^{1.5}
- o Projectile mass ~ 3 g
- o Acceleration $\sim 10^6$ m/s² $\approx 10^5$ g's
- o Barrel length ~ 1 m
- o Bore dimension ~ 1 cm
- o Muzzle velocity ~ 1 km/s. ^{1.4}
- o Force $\sim 3 \times 10^3$ N = 674 lb_f

The second section of this report describes the rail gun power supply; the third section describes the gun itself with its various components and the devices which measure its performance. The fourth section, in assessing the gun's performance, discusses the measured quantities and their significance.

II. POWER CIRCUIT

The rail gun presents a highly nonlinear load to the electrical circuit which must supply it with power. The inductance of the load varies with time, being very small initially and increasing as the armature is driven forward. The resistance is also nonlinear with components which reflect work done in accelerating the projectile, rail resistance and the potential difference across the armature. Since the force applied to the projectile varies as the

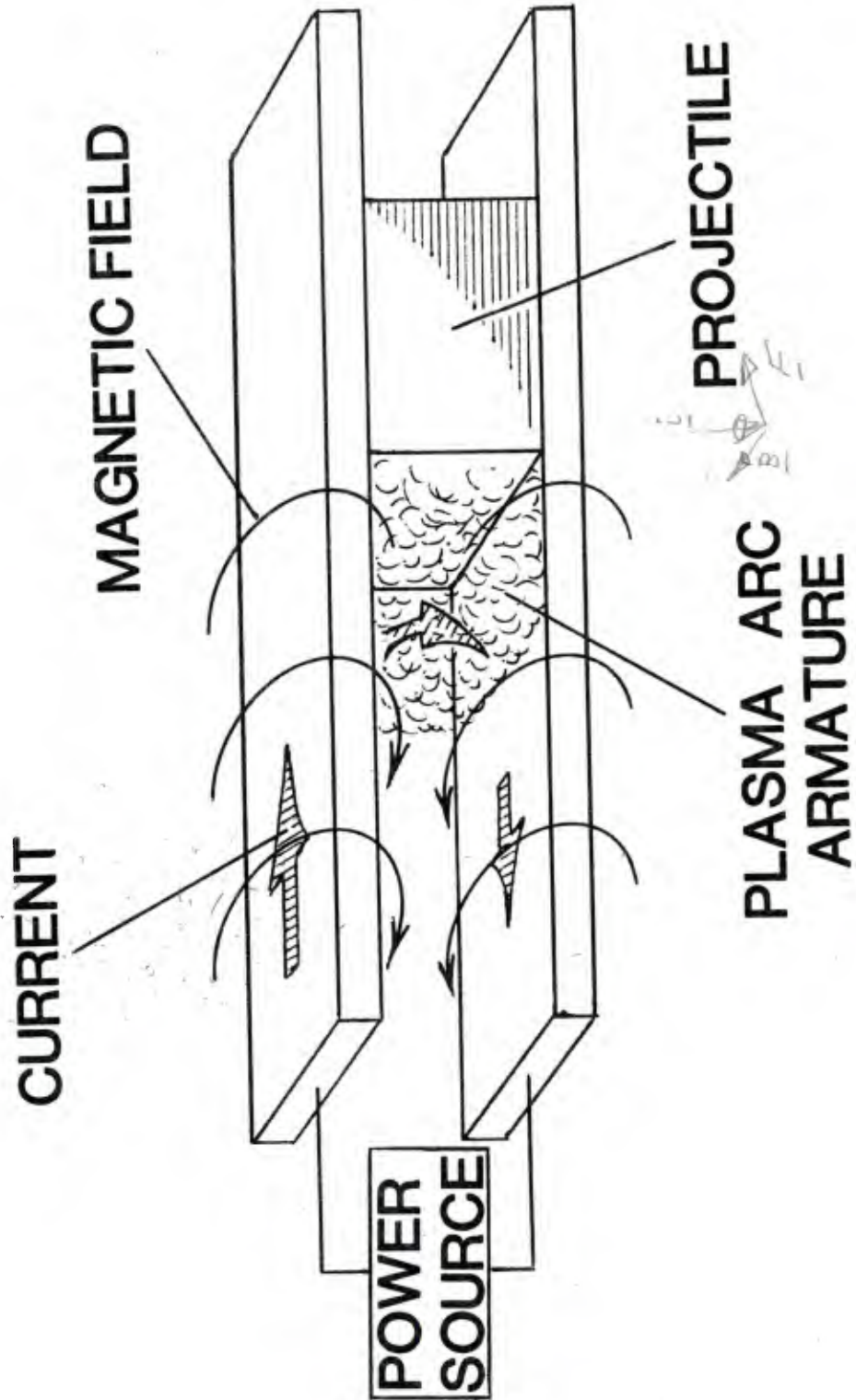


Figure 1. Rail Gun Schematic

current squared as in Eq. 1, an inductive power supply, which inherently acts to maintain currents irrespective of time-varying load, is the best choice for the rail gun's power supply. Current will, of course, be reduced as energy is drawn from the inductor but low impedance loads will not cause rapid, inefficient energy depletion as with a capacitive power supply.

The inductive power supply must have current established by another energy source. The group at the Australian National University⁴ has accomplished this by first "charging" a storage inductor with a homopolar generator (HPG) (which discharges too slowly to power a rail gun directly) and then connecting the inductor as the power source for a rail gun. We, too, use a storage inductor, but instead charge it with a capacitor bank (which discharges too rapidly to power a rail gun directly). The circuit for the power supply we have constructed is shown schematically in Figure 2. Its operational time sequence is as follows:

- o The capacitor bank is charged by an external power supply, typically to 9,100 V.
- o The trigatron switch closes allowing current to flow through the coil.
- o When the current is at maximum (i.e., when the largest amount of energy is stored as a magnetic field), the exploding wire acts as an opening switch.
- o As the opening switch begins to operate, a large inductive voltage is developed across the rails. An internal initiator then promotes electrical breakdown between the rails. This establishes an arc through which current flows from one rail to the other.
- o Current flow through the rails and the plasma arc armature causes the armature and projectile to be accelerated.
- o The driving force continues until either the projectile exits or the current diminishes to a value no longer sufficient to maintain an arc.

In the paragraphs that follow, each of the major components of the circuit is described in more detail.

A. Capacitor Bank

The initial energy storage is accomplished by a bank of twenty 6×10^{-5} F, 10,000 V, energy discharge storage capacitors. The inductance of each capacitor is 22.5×10^{-9} H and all are connected in parallel using RG 17 A/U coaxial cables. The shield of each cable is connected to the capacitor case and the center conductor to the capacitor electrode. All are charged at the same time from a single power supply. In practice we limit the charging to 9.1 kV or 50 kJ of total stored energy.

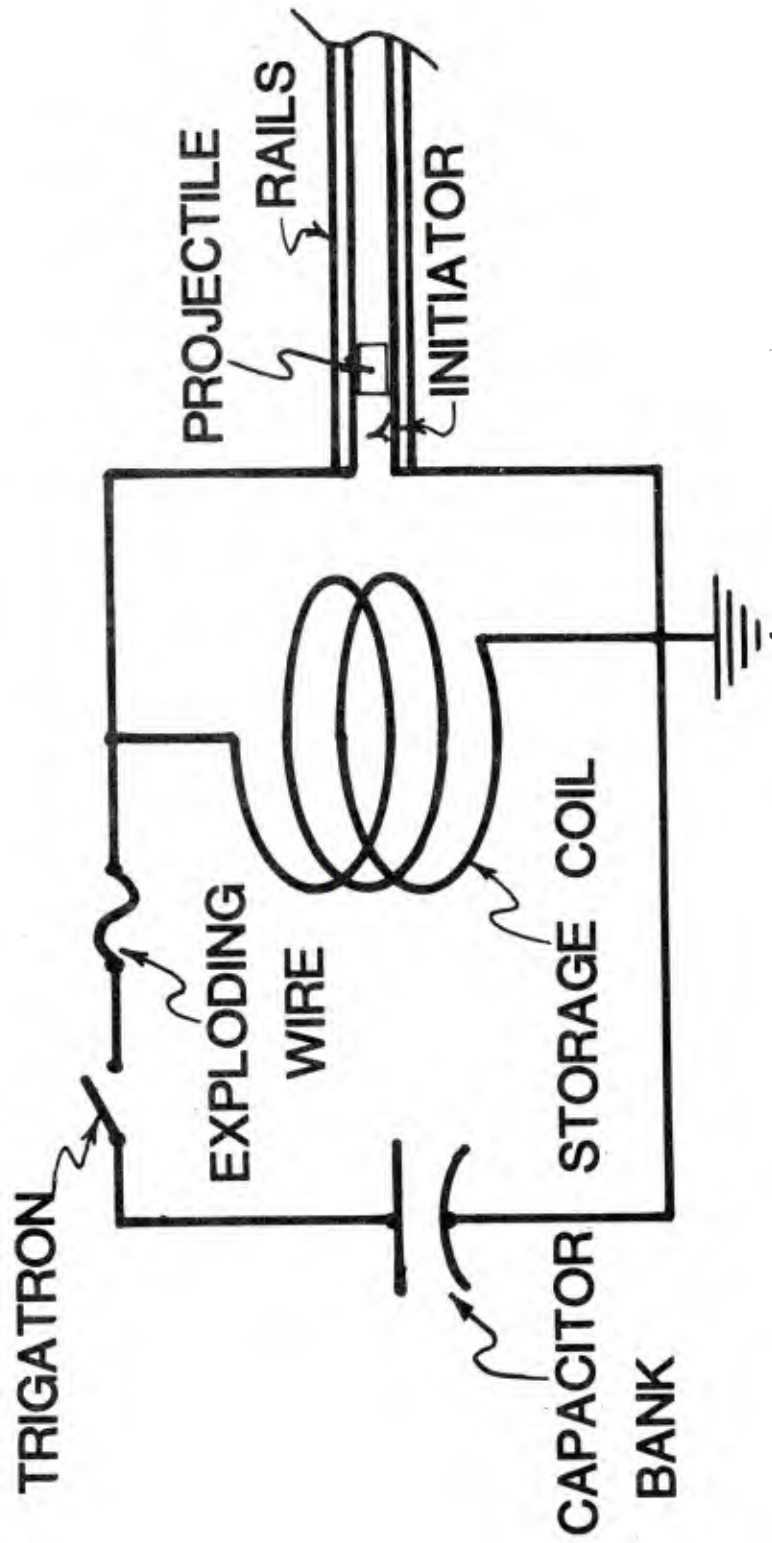


Figure 2. Intermediate Inductive Storage Circuit

B. Storage Coil

The intermediate energy storage is in the form of a magnetic field linking a coil. The coil is a tightly wound, right cylinder consisting of three, parallel, size 000, stranded copper cables. Each cable makes 3-1/2 turns around a 1.5 cm thick, cylindrical Plexiglas form 19 cm in diameter; each winding start is offset by 120° for symmetry. The entire winding is potted in polyurethane and reinforced with an outer, polyurethane kevlar wrapping.

The inductance has been calculated by the Nagaoka formula⁹ to be 1.7×10^{-6} H. The energy stored in an inductor's magnetic field is given by

$$E = \frac{1}{2} L_s I^2 \quad (2)$$

where L_s is the inductance and I is the current.

C. Closing Switch

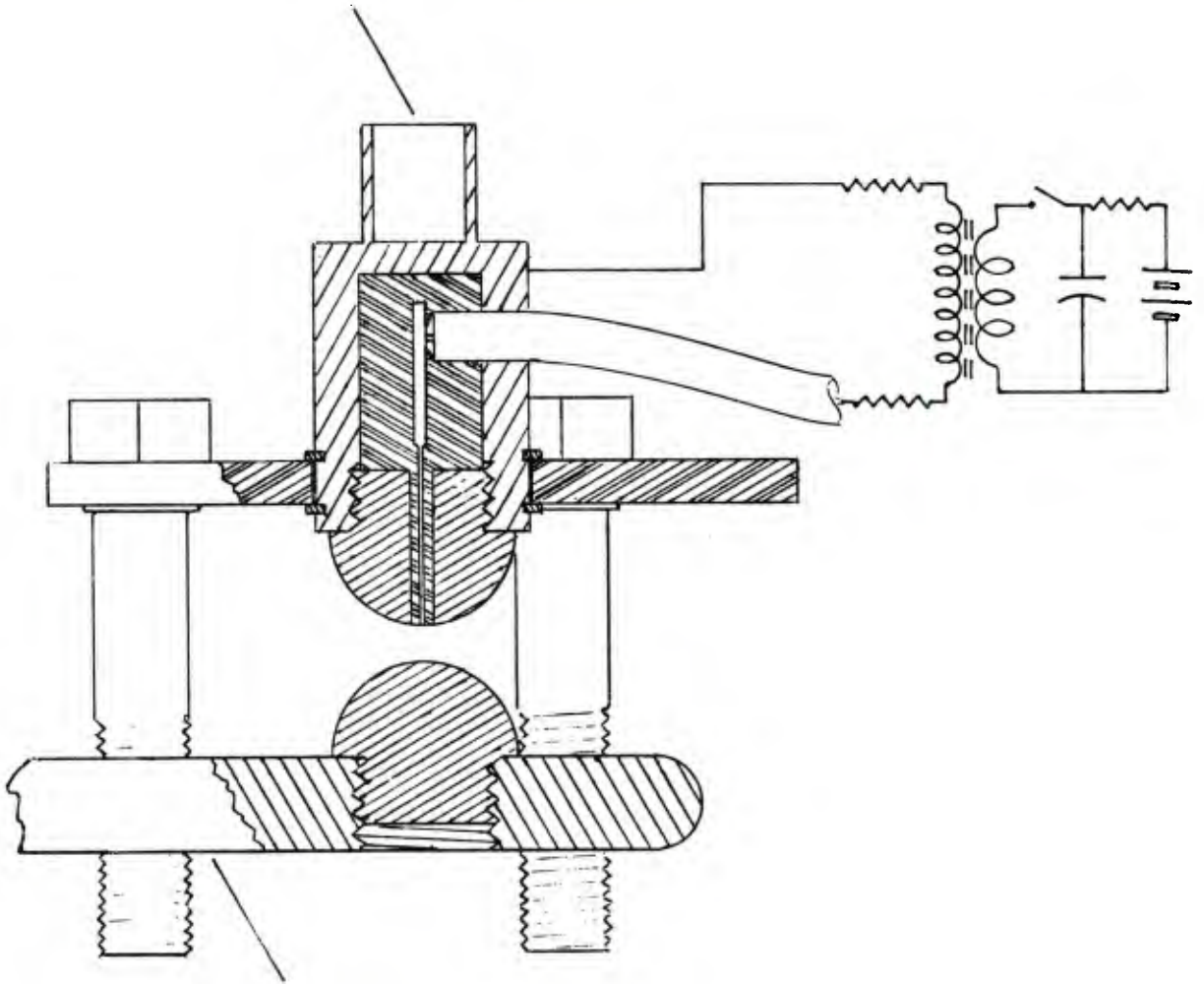
The trigatron closing switch and associated circuit are shown in Figure 3. When the capacitor bank is fully charged, the trigatron is remotely activated to discharge the capacitors through the storage inductor. The electrodes are tungsten hemispheres; the upper one is drilled axially to accommodate a teflon rod with a brass wire core. The brass wire is connected to one of the high voltage leads of a step-up transformer. The other lead is connected to the upper electrode so that, when triggered, a spark jumps from the inner brass wire radially outward to a point on the upper electrode. The resulting disturbance is enough to cause electrical breakdown between the lower and upper electrodes. This breakdown results in an arc which maintains about a 200 V drop independent of the current flowing through the triggered gap. Current continues to flow for about 85 microseconds until the exploding wire opens the circuit; at this time the trigatron discharge is extinguished, and the capacitors are no longer connected in the circuit.

D. Opening Switch

To accomplish this high current switching operation, an exploding wire was chosen. (See Figure 2.) The switch must sustain an increasing current for several tens of microseconds and interrupt this current at the peak. The opening switch action is achieved by the production of a long column of copper vapor too diffuse to provide metallic conduction and too dense to permit avalanche ionization. Because such a high pressure column expands rapidly, the switch can remain open only a short time before expansion to arc supportive densities occurs. This expansion may be slowed by the inertia of added mass; such mass has been provided by a jacket of sand (glass beads) as shown in Figure 4. The timing of the switch is directly related to the time to generate the heat of vaporization at the rate $I^2 R_w$. When the current is initiated, the major circuit voltages are found across the capacitor and the inductor; current and wire resistance are both low. The LC combination allows current to rise

⁹F.W. Grover, Inductance Calculations, D. Van Nostrand Co., Inc., NYC, 1946.

To Exploding
Wire Holder



To Capacitor Bank
High Voltage Lead

Figure 3. Trigratron Closing Switch

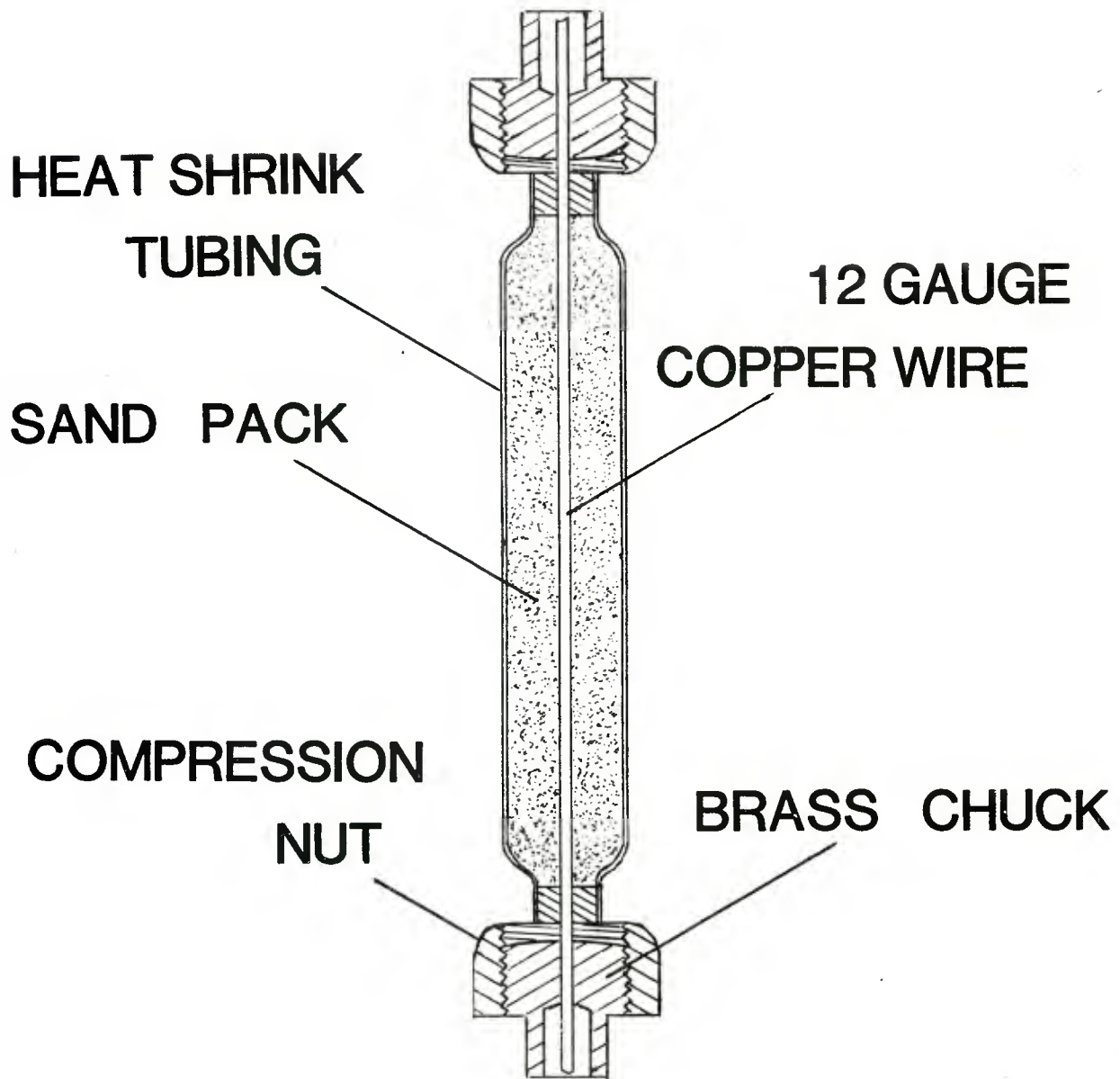


Figure 4. Exploding Wire Opening Switch

and the resultant ohmic heating raises the wire's resistance. The rate at which energy is supplied to heat the wire, $I^2 R_w$, thus rises more and more rapidly. When the wire temperature is high enough, surface vaporization begins, causing the effective wire cross section to diminish, thus further increasing the rate of resistance rise. At the time when the switching begins, the wire resistance has become the major impediment to current while (with proper timing), the capacitor voltage, has dropped to near zero. The negative current derivative reacts with the inductance to produce an increasingly large voltage opposing the current change. This voltage eventually becomes sufficient to break down the gun initiator gap. (See Figure 5.) Current now follows the resulting new, low impedance path, decaying slowly so that voltage across the inductor becomes a few hundred volts with loss of current. In the capacitor circuit, ionization within the vapor column decays and permanently opens the switches. It should be noted that the energy to operate the opening switch is about 40% of the initial stored energy.

An improper choice of exploding wire length or gauge results in a "ring back," in which the exploding wire opening switch recloses, reconnecting the capacitor bank to the inductor. To choose more accurately the gauge of the wire to be used, a short computer program (Appendix A) was written to model the capacitor, exploding wire, inductor circuit. This resistive heating program links resistance of the wire to (a) thermal resistance increase and (b) cross section reduction by loss of vaporized material. When the calculated value of the energy dissipated by the wire's resistance equals the value needed to completely vaporize the total mass of the wire, the program considers the switch open and terminates. Though all of the values used in the program are approximate, the output is sufficiently accurate to avoid guesswork in finding a proper exploding wire.

Details of the exploding wire assembly are shown in Figure 4. The exploding wire was held at each end by jaws formed by three diametric saw cuts across the taper-threaded end of a brass rod. The wire, parallel to the rod's axis, was inserted at the intersection of the saw cuts. A compression nut, tightened onto the taper thread, drew the jaws tightly against the wire. This assembly was then hose-clamped into the circuit.

E. Arc Initiator

The arc initiator (gun closing switch) is shown in Figure 5. This switch is an "L"-shaped piece of foil, resting on the lower gun rail with a specified gap between the vertical tip and the upper rail. When the exploding wire begins to choke off the current in the capacitor-inductor circuit, the large time rate of change of current produces a large voltage drop across the coil. This voltage drop also appears across the initiator gap and causes electrical breakdown when the voltage is large enough. The current flowing through the closing switch is sufficient to vaporize the foil and create the plasma arc armature for the rail gun. The current in the rails has associated with it a magnetic field which interacts with the current in the arc, producing the force which accelerates the arc and projectile. To ensure that the gradient dL/dx producing force on the arc is not influenced by rail-end effects, the initiator switch is placed 10 cm in from the breech end of the gun.

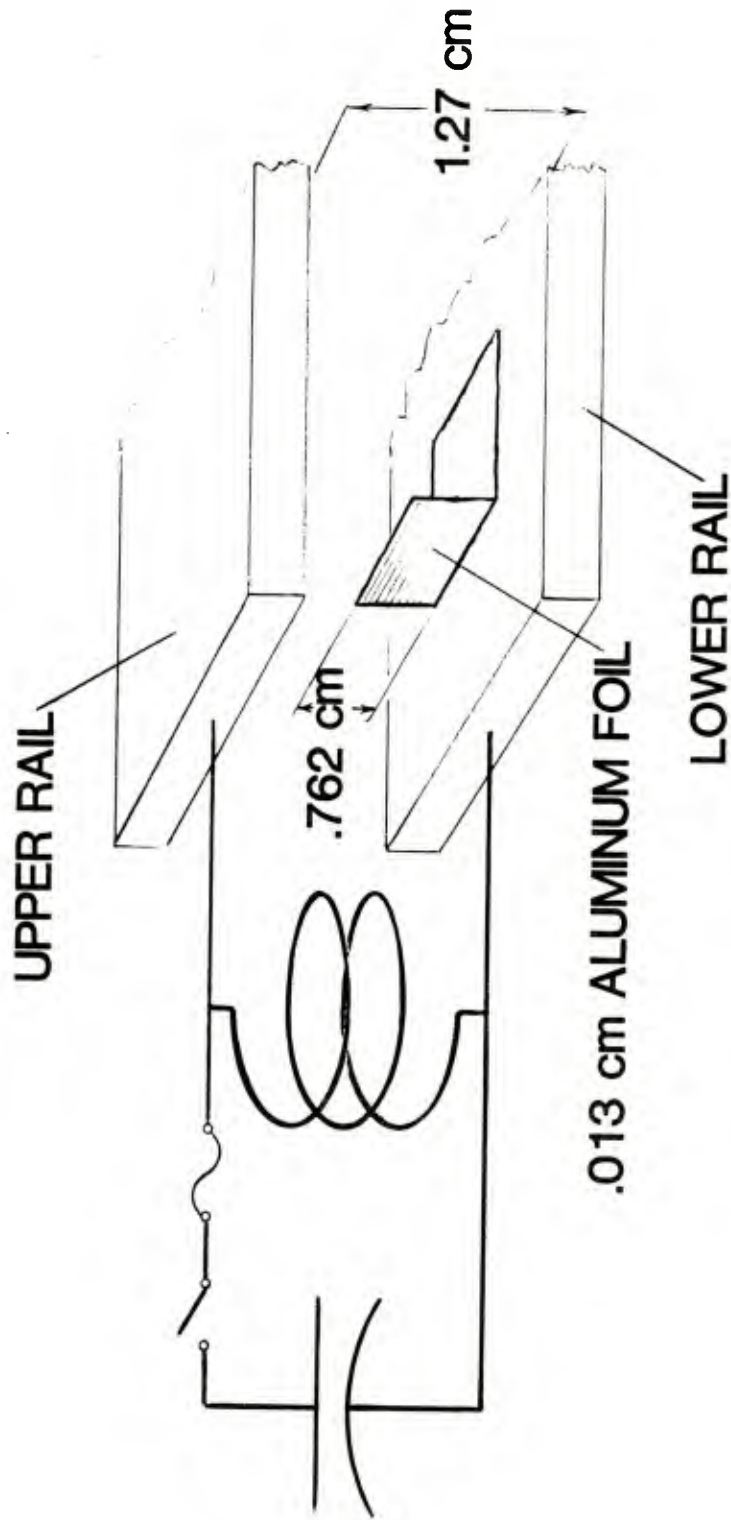


Figure 5. Arc Armature Initiator

F. Connections

To allow flexibility in mechanical variations of the circuit all connections are clamped rather than soldered or welded. Soldering may produce extra contact resistance with consequent ohmic losses. Welding is probably the best method of making connections but is far too inflexible for a laboratory device. The upper and lower rails are each drilled for "U" clamp draw bolts to pressure-connect their respective cables. Other circuit connections are clamped with common hose clamps. When the contacts are clean and tightly bound no evidence of arcing or burning is found; loose connections very often show signs of arcing.

Care was taken on the initial hookup of the inductance coil to have the leads extremely clean, even to the point of vacuum sputtering the ends of the cable and vapor depositing a thin layer of gold to reduce oxidation. After many disconnect-reconnect cycles, there is visible evidence that much of the gold remains in place.

III. RAIL GUN

A. Design Features

The gun, a 1 metre long, square bore tube open at both ends, was designed for easy assembly and dismantling. A view of the assembly is shown in Figure 6. The 0.635 x 2.54 cm copper rails, cut and machine-smoothed from 1/4" copper plate, formed the upper and lower walls of the tube; T-sectioned melamine bars formed the side walls and served to space and align the copper rails. The inner dimensions of the bore were 1.270 x 1.270 $\begin{matrix} +0.003 \\ -0.000 \end{matrix}$ cm. The rail-over-rail configuration provided gravity hold down of parts to facilitate assembly and also allowed horizontal orientation of instrumentation for measurements transverse to the arc current flow. Holes were drilled in the melamine bars to hold fiber optics and to pass laser beams; flux sensing coils were epoxied in grooves on the outside of the bars. The inductance of the 1 metre loop formed by the assembled bore and the arc armature was calculated^{9,10} as 0.51 μH . The stresses on the gun and the force on the bullet were calculated using Eq. 1 with x representing distance in the direction of the desired force.

Because the force driving the bullet is actually built up in the conducting gases of the arc, these gases transmit a hydrostatic force to the melamine sidewalls also, necessitating their constraint. The bi-directional constraint was achieved by clamping the rail and sidewall assembly between a pair of steel angle beams as shown in Figure 6. Insulating polyurethane strips filled the volume between the angle beam and the gun tube. Each polyurethane strip was cast in an aluminum tray which restrains its tendency to spread under the wedge action of the gun tube corners. (See Figure 6.) The aluminum also provides low friction against the steel to facilitate slippage as the polyurethane casting comes into correct alignment during tightening. C-clamps, with

¹⁰ Frederick E. Terman, Radio Engineers Handbook, 1st Ed., McGraw-Hill, NYC, (1945), p. 53.

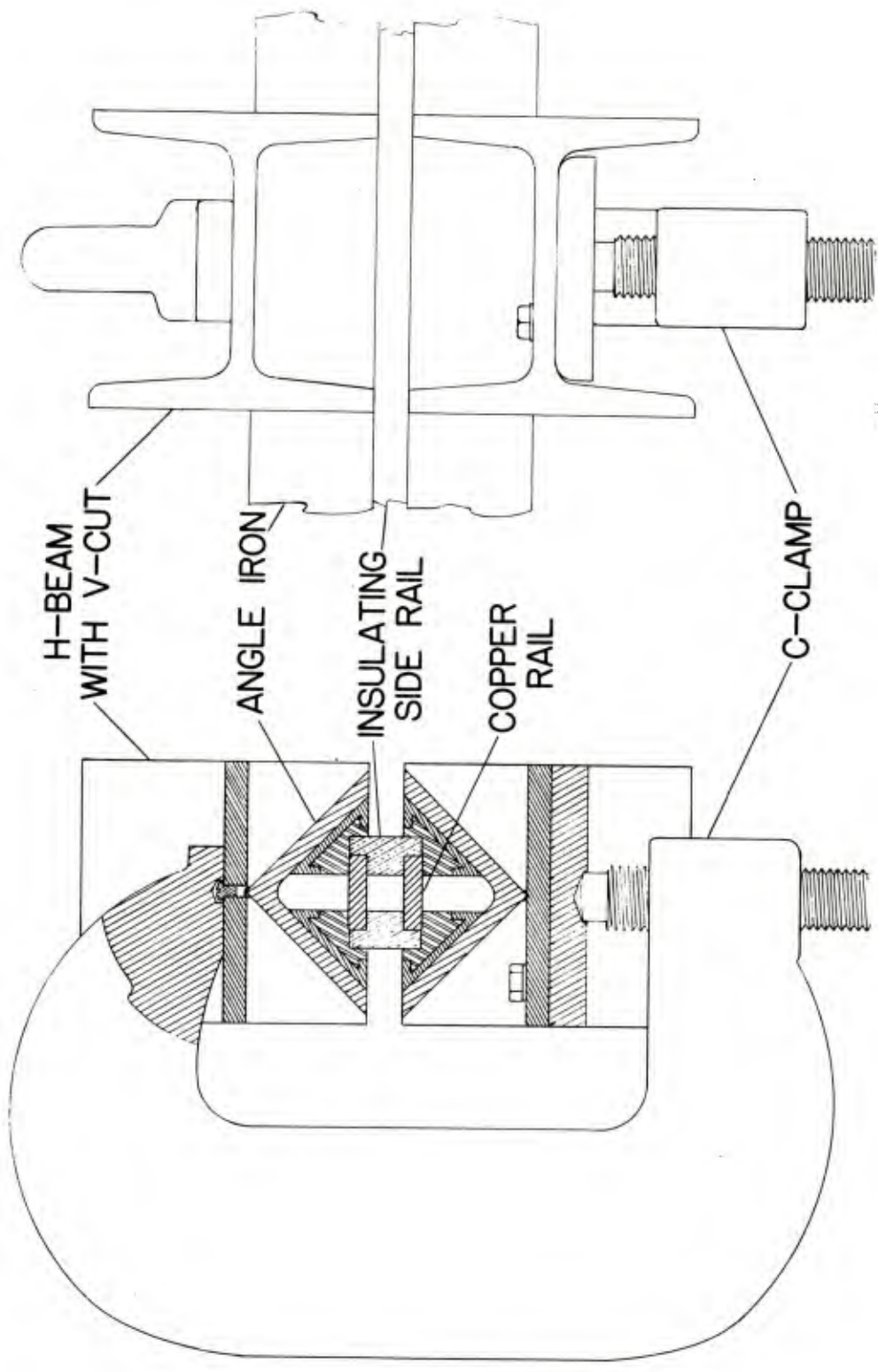


Figure 6. Cross Section View of Barrel Assembly

aligning guides to direct the application of force, hold the gun together. As the capacitor bank size was increased from 300 to 1200 μF , stiffeners cut from aluminum H-beams were added to prevent the angle beam from opening up and allowing venting of bore pressure.

B. Projectiles

The arc armature exerts a hydrostatic force on the rear of the projectile. As a result, some care must be taken in the areas of projectile-to-barrel sealing and in-bore dynamics. In our early attempts, a simple 12.7 mm cube of lexan polycarbonate was used as the projectile. Disassembly of the gun after firing revealed a thin layer of black soot on all the inner surfaces of the barrel. The soot was relatively uniform except for several small regularly spaced areas where the surface had been wiped clean. We attributed these markings to projectile balloting in-bore. In addition to a lack of projectile stability, this observation and its assessment imply a leakage of arc material past the projectile. Without such blow-by prior to passage of the projectile there would have been no material in which to write ballot marks.

A study on projectile balloting¹¹ suggested three design improvements to the projectile. The first was to lengthen the projectile; a cube, of course, has a length of one caliber, which is too short. The second was to move the center of gravity towards the rear of the projectile. This is easily accomplished in our case simply by drilling out the leading surface of the projectile. The third suggestion was to provide better projectile-to-barrel sealing and to make this seal as near to the rear of the projectile as possible. All three suggestions were incorporated into the design of the final projectile which is a 12.7 x 12.7 x 19.0 mm block with a 9.5 mm hole drilled into the leading surface to a depth of 12 mm. A 1 mm thick 12.75 x 12.75 mm neoprene pad was glued to the rear surface so that its edges bear against the inner surfaces of the bore. The improved projectile has a mass of 2.8 grams. In practice the projectile was sanded down to about .05 mm less than the bore dimension. This size was determined by sanding and then pushing the projectile down the entire length of the barrel repeatedly until very little force was needed to move the projectile in the bore. Further tests with this projectile showed no evidence of soot on the front of the projectile after firing and soft recovery.

IV. MEASUREMENT DEVICES

The four measurement devices described in this report have collectively had a dual function. The first was to measure the performance of the gun throughout its development. The second was to characterize the arc armature in the general terms of energy, current, voltage and velocity. The measurement techniques and the rail gun evolved in the same time frame.

¹¹K. Fansler, "On Balloting of Projectiles," ARBRL-MR-02831, April 1978 (AD A055707).

A. Fast Rogowskii Coil

A time varying electrical current can in principle be measured by sensing the magnetic field in the vicinity of the current, integrating the resulting signals and multiplying by a geometrical factor. The Rogowskii coil^{12,13} operates on exactly this principle. Being toroidally wound, however, it has the unique advantage that its mutual inductance, M , with a current carrying circuit is fixed, regardless of the relative orientation, as long as the circuit links the torus once. It samples the time rate of change of the magnetic field along a closed path. The relation between the sensing coil's voltage, $V(t)$, and the current, i , to be measured is given by the differential form of Ampere's circuital law:

$$V(t) = M di/dt \quad (3)$$

The signal from the Rogowskii coil can be electrically integrated with an RC two-port filter to give an output proportional to the measured current. The RC two-port filter is characterized by two limiting frequencies, an upper one beyond which its response droops and a lower one beyond which it cannot properly integrate the time differential. The upper limit frequency response of our RC two-port filter is 1.1 MHz and the lower limit is 450 Hz. Measurement accuracy is poor at the extremes of the range set by these limits. A compressed range over which accuracy is best is customarily defined with the lower and upper limits 10 and 1/10 times the characteristic frequency limits, respectively. The resulting values, 4500 Hz and .11 MHz, correspond to event durations in the range of 220 to 9 μ s.

The sensing coil with its RC two-port was calibrated as a unit by looping a circuit carrying a known current through the torus and monitoring both the current pulse and the voltage output of the RC two-port. The measured sensitivity of 70,000 amps/volt compares very favorably to a calculated value of 60,000 amps/volt based on an approximated mutual inductance and the computed response of the RC two-port.

The fast Rogowskii coil was placed around the ground-side return lead from the inductive storage coil to the capacitor bank. Its position in the power circuit can be seen in Figure 7.

B. Voltage Divider

To measure the large, rapidly varying voltage across the breech of a rail gun with an oscilloscope or waveform digitizer a low inductance, resistive divider was needed. The 100:1 divider chain was chosen to be 2000 ohms with the

¹² Adolf J. Schwab, *High Voltage Measurement Techniques*, MIT Press, Cambridge, MA (1972), p. 180-186.

¹³ D.G. Pellinen, M.S. Di Capua, S.E. Sampayan, H. Gerbracht and M. Wang, "Rogowskii Coil for Measuring Fast, High Level Pulsed Currents," *Rev. Sci. Instrum.* 51, 1535 (1980).

measurement taken across the final 20 ohms. The position of the voltage divider is shown in Figure 7. The base of the chain is connected to the ground point of the gun and power circuit. A 50 ohm coaxial signal cable was connected across the 20 ohm resistor with its grounded shield also serving as the sole ground for the recording device. Coaxial leads from the probes to the recording instruments are necessary to reduce the inductive pickup of stray fields. Single point grounding is essential since significant voltage (in series with the true signal) will be developed across any probe leads that are part of a ground loop enclosing stray, transient fields. To protect the recording instruments a zener diode was placed across the oscilloscope signal terminals. The diode restricts the scope input to voltages between zero and minus seven volts.

C. Slow Rogowskii Coil

The current pulse through the rails and armature has a much longer time duration than does the capacitor discharge current. To measure this current we need a slightly different sensing coil and a much longer integrating RC two-port filter. The time constants for the probe were chosen to be .5 microsecond and 2200 microseconds for the rise and fall times of the coil and integrator combination. The integrated signal should be valid for times from 5 to 220 microseconds. The slow Rogowskii probe was calibrated in a fashion similar to the fast Rogowskii probe described in segment A of this section. Its calibration constant, 500,000 amps/volt, shows that it is far less sensitive than the fast probe. The reduced sensitivity is a consequence of the increased decay time of the RC two-port.

The position of the slow Rogowskii coil monitoring the arc (rail) current is shown in Figure 7. It encircles the lead from the inductance coil to the upper rail of the gun. In this position no current is measured until the arc armature has been initiated.

D. Ballistic Pendulum

To measure the exit velocity of the projectile a ballistic pendulum was constructed. A cylindrical catch tank weighted with lead bricks, total mass 30.0 kilograms, was hung by a four-wire suspension from a fixed frame. A felt-tipped pen, attached horizontally to the catch tank with its point against a fixed paper, recorded the displacement of the pendulum. The displacement was used to calculate the final velocity of the projectile, typically 1.2 km/s. For safety, the catch tank completely covered the end of the barrel. Unfortunately, this added the momentum of an undetermined mass of hot gases associated with the discharge of the gun to that transferred to the pendulum by the projectile.

V. PERFORMANCE

The rail gun's performance is monitored by the devices described in the preceding section. The quantitative information extracted pertains to the flow of energy and is derived from the charging voltage, two current measurements and the ballistic pendulum. The voltage divider provides a time history

of the breech voltage which is primarily qualitative in descriptive value since this voltage is the sum of several independent components.

A. Breech Voltage

The voltage drop across the breech of the rail gun is, as may be seen from Figure 7, also the voltage developed across the storage inductor. As such, it gives a history of the entire gun discharge event. Figure 8 is a typical record with indications of each of the steps in the energy transfer and conversion process. The early positive spike, starting at the activation of the trigatron closing switch, represents the voltage developed across the storage inductor as the current rises in the capacitor circuit and energy is stored in the magnetic field of the storage inductor. This voltage reaches the initial capacitor charging voltage but forward conduction of a protective zener diode has severely limited the oscilloscope signal.

The negative inductive spike (at $\sim 90 \mu\text{s}$) occurs as current is shut off by the exploding wire opening switch and may reach -20,000 volts. The resulting signal at the oscilloscope is limited by the avalanche conduction of the protective zener diode. The voltage amplitude then diminishes to -300 volts as the arc "strikes" between the initiator and the upper rail. The amplitude continues to diminish but at a slower rate to -200 volts as the arc becomes established; the oscillations observed probably reflect inductive effects or possibly multiple strike points as several small arcs try to establish themselves. The voltage then decays slowly to -100 volts as the arc proceeds down the rails and consumes the inductively stored energy. A small spike at the end of the trace indicates the exit of the projectile and arc.

The voltage between the upper and lower rails at the breech of the gun is the result of resistive drops and changing fluxes in the current flow loop defined by the rails and the advancing arc armature. The breech voltage may be described as

$$V_{\text{BREECH}} = V_A + V_R + V_{\phi} \quad (4)$$

where the voltage across the armature, V_A , is on the order of 150 volts. Its value is remarkably constant over the observed range, 20,000 to 180,000 A; this is evidence of its highly nonlinear character as a power circuit load. Sources of potential drop which may contribute to this voltage are the ionization potential of the armature materials, some type of contact effect existing at the rail-plasma interface, and a boundary layer of low conductivity attributable to cooling by the adjacent, massive copper rails. The single-ionization potentials for Al and Cu are about 6.0 and 7.7 V, respectively. We expect contact effects to be on the order of work function voltages, which are small and may even cancel over the two interfaces. Boundary layer effects can be predicted only with detailed knowledge of the fluid dynamics at the high temperatures, pressures, and velocities experienced.

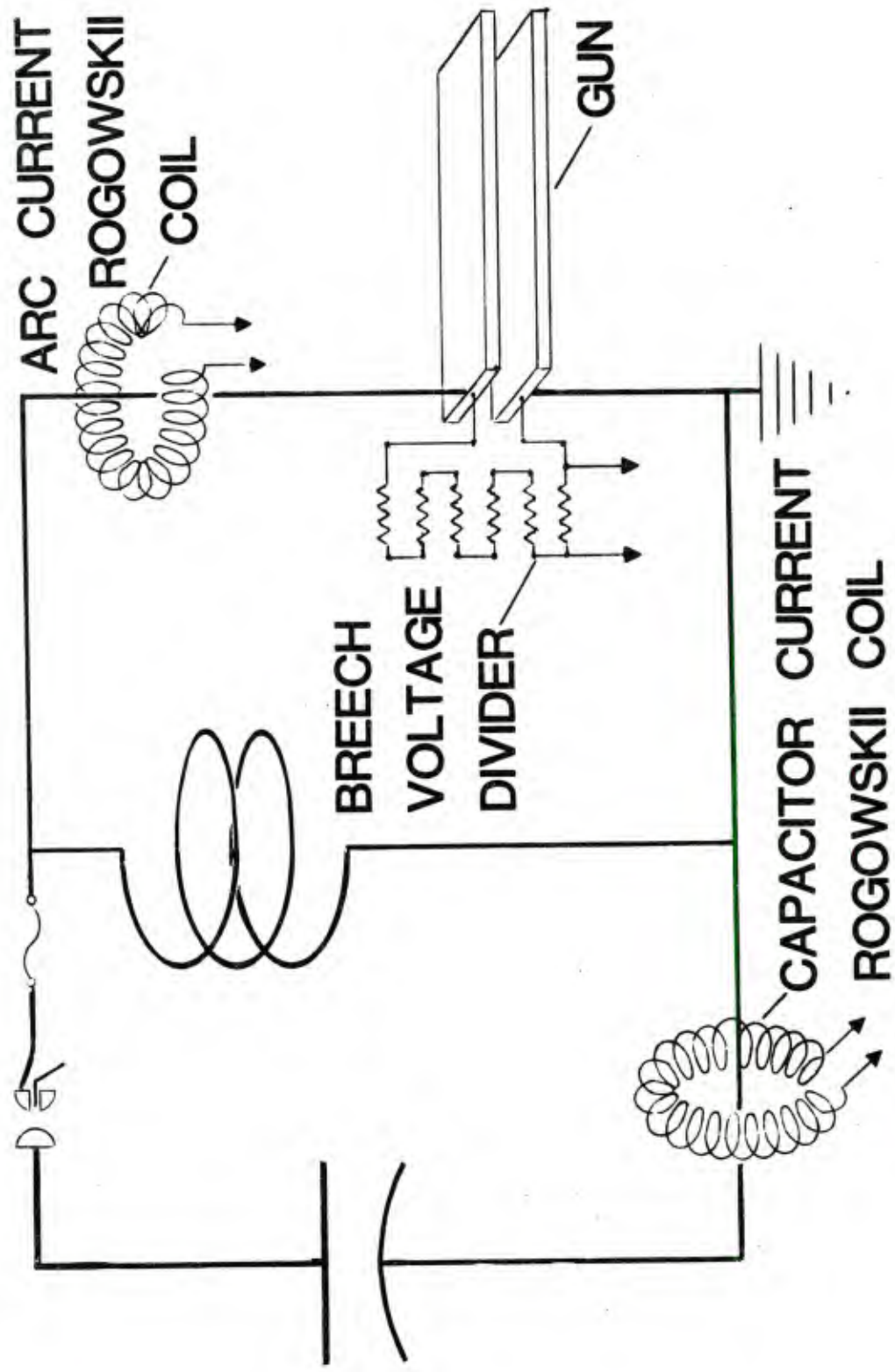


Figure 7. Location of Measurement Probes

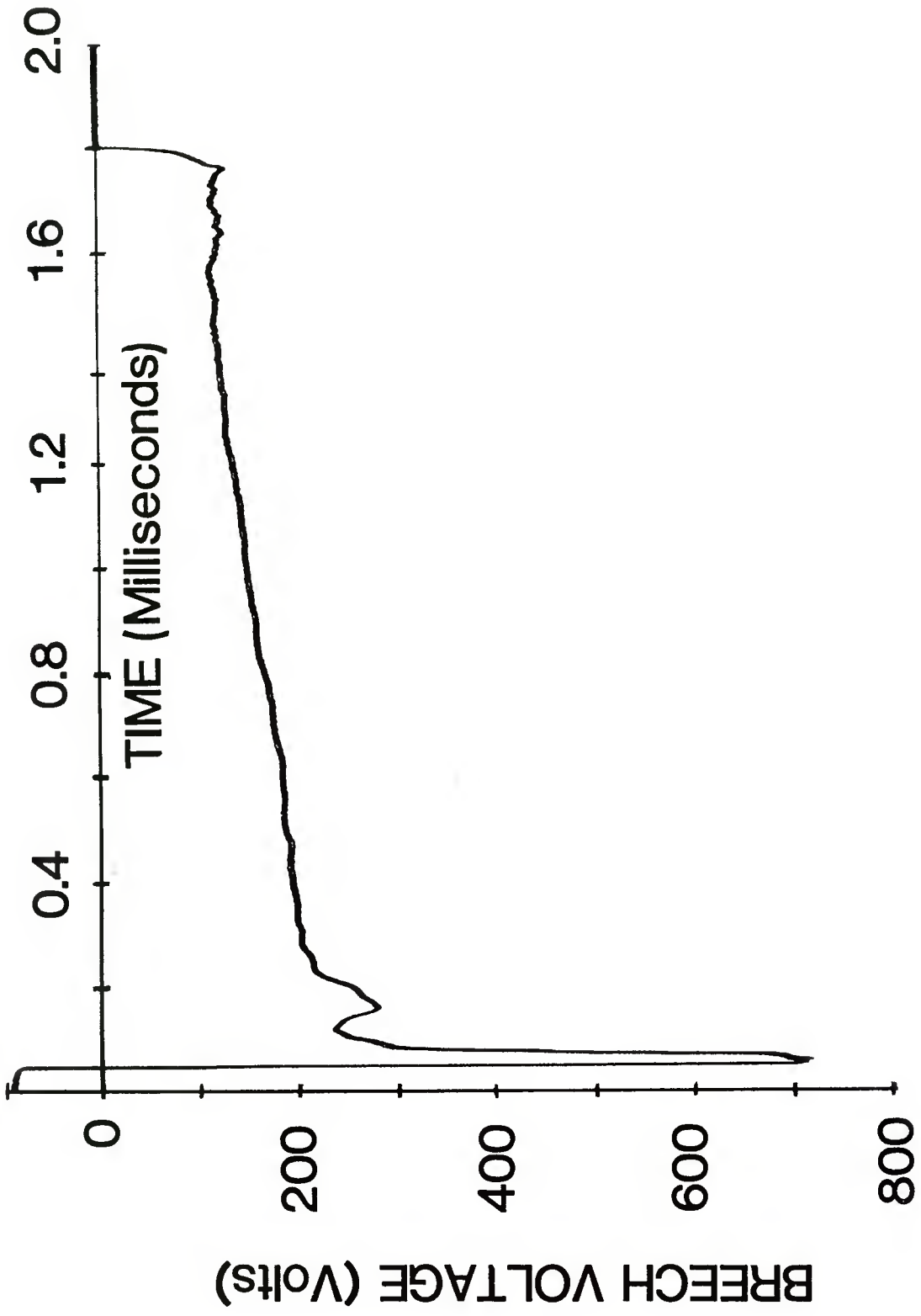


Figure 8. Breech Voltage Versus Time

The total potential drop along the two conducting copper rail segments, V_R , is a nearly negligible fraction of the breech voltage. The length of each segment is the distance between the location of the measurement and the arc position. The maximum total length is 2 metres which corresponds to a resistance for nonvarying currents (uniform depth distribution) of 0.23 milliohm. With a projectile-exit current of 20,000 A., this would create only a 5 volt IR drop along both rails. Because the traveling armature continuously establishes current flow in new parts of the rail, transient skin effect limits the rate of penetration of current into the 6.3 mm thick rails and a distribution of current exists whose depth at each location is a function of the time since local turn-on. As an approximation, a mean value of penetration was taken to be the 1 kHz skin depth, 2.4 mm; the corresponding IR drop at exit would be 12 V. Similar results using more detailed calculations confirm that the resistive drop in the rails accounts for only a small portion of the observed breech voltage signal.

The changing flux through the expanding loop made up of the voltage divider, the arc armature, and the two rails produces a voltage across the voltage divider

$$V_{\phi} = - \frac{d\phi}{dt} = - i \frac{dL_{\ell}}{dt} - L_{\ell} \frac{di}{dt} \quad (5)$$

where L_{ℓ} is the instantaneous inductance of the rail pair section between the voltage divider and the armature and $\phi = L_{\ell}i$ is the magnetic flux.

As the armature advances, the current established in new portions of the rail produces flux to fill the expanding loop. This part of the flux change is expressed by the first term of the right-hand member of Eq. (5). The second term expresses the effect of the large decay rate of the gun circuit current. Because all of the terms are changing with armature travel, Table 1 is given to list approximate conditions near the start of this travel and near the end. The net voltage due to changing flux is evidently small and not a significant fraction of our observed breech voltage.

The above considerations show the breech voltage measurement to be dominated by the potential drop across the armature and its interface to the rails. The arc corresponding to our observations may be represented by about one milliohm of resistance in series with a constant, current-independent 100 V potential.

B. Capacitor Discharge Current

The discharge of the capacitor bank transfers and converts stored electrical energy to magnetic field energy of the intermediate storage inductor. The expected capacitor discharge current is roughly sinusoidal until the exploding wire breaks the current at the quarter cycle point. The signal from the fast Rogowskii coil probe for a typical capacitor discharge/inductive energy storage event is shown in Figure 9. The current shows close adherence to the sinusoid until about 85 microseconds, at which time the resistance of the exploding wire has become so great that the current is broken. For a typical shot, 50 kJ of energy is stored in the capacitor bank, as determined by:

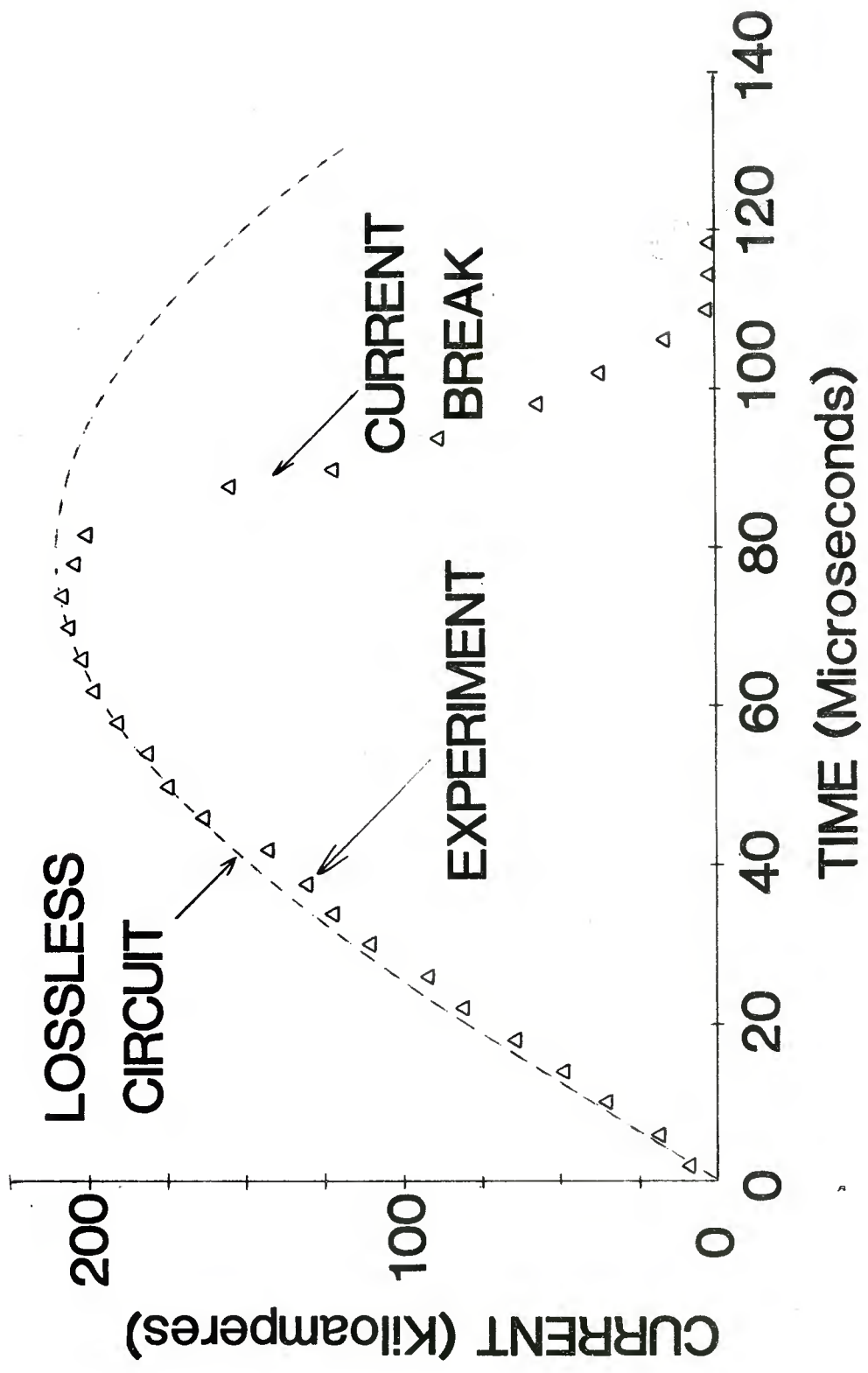


Figure 9. Capacitor Discharge Current Versus Time

TABLE 1. FLUX CHANGE CONDITIONS

$$\frac{d\phi}{dt} = L_{\ell} \frac{di}{dt} + i \frac{dL_{\ell}}{dt}$$

	ARMATURE NEAR <u>BREECH</u>	ARMATURE NEAR <u>MUZZLE</u>
Velocity	10^2 m/s	10^3 m/s
i	1.5×10^5 A	2×10^4 A
L_{ℓ}	4×10^{-8} H	4×10^{-7} H
$\frac{di}{dt}$	-2×10^8 A/s	-3×10^7 A/s
$\frac{dL_{\ell}}{dt}$	4×10^{-5} H/s	4×10^{-4} H/s
$L_{\ell} di/dt$	-8v	-12V
$i dL_{\ell}/dt$	6V	8V
$d\phi/dt$	-2V	-4V

$$E = \frac{1}{2} CV^2$$

(6)

where C, the capacitance of the bank, is 1200 μ F and V, the initial voltage charge, is 9100 V. As the bank discharges through the storage inductor, a peak current of 210,000 A is recorded. Substituting this current value and a circuit inductance value of 2.2 μ H inferred from the ringing frequency into Equation (2), one predicts 48.5 kJ of energy stored in the magnetic field linking the circuit and its components. The 1.7 μ H calculated inductance of the storage coil is 75% of the circuit value inferred. The remainder of the inductance is in the capacitors, switches, and hookup leads. From the 48.5 kJ of magnetic field energy, approximately 20 kJ are expended to vaporize the exploding wire used as an opening switch. There are additional small losses due to resistance in the circuit, which may be neglected.

> 97% stored in mag field

C. Arc Current

Just as the exploding wire is completing vaporization and the capacitor current is rapidly dropping toward zero, an arc is initiated in the rail gun and current begins to flow in the gun side of the circuit. The rail current starts up very rapidly, increasing from zero to 155,000 A in a few microseconds. When the rail current peaks, approximately 20 kJ of energy is stored in the magnetic field of the coil. The current versus time can be followed, noting that an inductor-resistor (L-R) series circuit exhibits an exponential

decay. Our measured current is shown in Figure 10 and decays approximately as an exponential with time constant, L/R , of 760 μ s. In a discharging rail gun, inductance and resistance increase as a function of time. The increase in inductance is due to the longer current path as the arc moves down the rails.

The resistance also increases with the longer current path and the mechanical work done by the circuit may be thought of as reflecting an added resistive term whose value varies with velocity.

As time evolves all of the energy stored in the coil's magnetic field is dissipated either to kinetic energy of the projectile, magnetic field between the rails, or circuit losses. For our small scale rail gun the circuit losses dissipate the major portion of the energy.

D. Velocity

The exit velocity of the projectile is measured by the ballistic pendulum and is also calculated from the known forces within the gun. Equation (1) defines the force which, if divided by the mass and integrated in time, yields the velocity. We have determined the velocity by both techniques for six firings. The result from the ballistic pendulum is a velocity of 1240 ± 90 m/s. The muzzle velocity as calculated from the measured current is 1070 ± 120 m/s. There is at least one systematic error in each measurement for which correction is not made: (a) the ballistic pendulum also receives momentum from the air in the barrel ahead of the projectile and the arc products following the projectile, and (b) the quasi-static value of dL_r/dx used to calculate the acceleration is probably too large because of transient skin depth effects. Because the mass of the air column in the gun tube ahead of the bullet is 7% of the mass of the bullet, a correction for the blast effect on the ballistic pendulum should give no more than a 7 percent reduction in the measured velocity. Other researchers¹⁴ have measured the inductance per unit length of various rail pair geometries as a function of frequency. They typically find a 10% reduction in dL_r/dx when the frequency is increased from 1 to 100 kHz. Thus, calculations based on measured current and a quasi-static dL_r/dx appear to slightly overestimate the integrated force and the resulting velocity. An average of the two values yields a value for the velocity of 1160 m/s. At this velocity a 2.8 gram projectile carries 1.9 kJ of kinetic energy. The overall transfer and conversion of energy from the capacitor bank to the projectile is 3.8 percent efficient.

at 50% eff $V_0 = 4.2$ km/s (13,800 f/s)

The rail gun is the least efficient energy conversion link in the power train. Of the 20 kJ supplied to the rails the yield is only 1.9 kJ of kinetic energy for a final stage conversion efficiency of only 9 percent. Arc losses, which dominate our system, do not increase linearly with increasing currents; thus, a large, higher current rail gun will have improved efficiency. The present system does, however, provide a plasma arc which is driven the full 90 cm of the rail gun. This performance meets our requirements for diagnostic studies of driven plasma arc armatures.

¹⁴I.R. McNab, et al., "DC Electromagnetic Launcher Development: Phase I," Contractor Report ARLCD-CR-80009, May 1980, AD-E400 419, p. A-47.

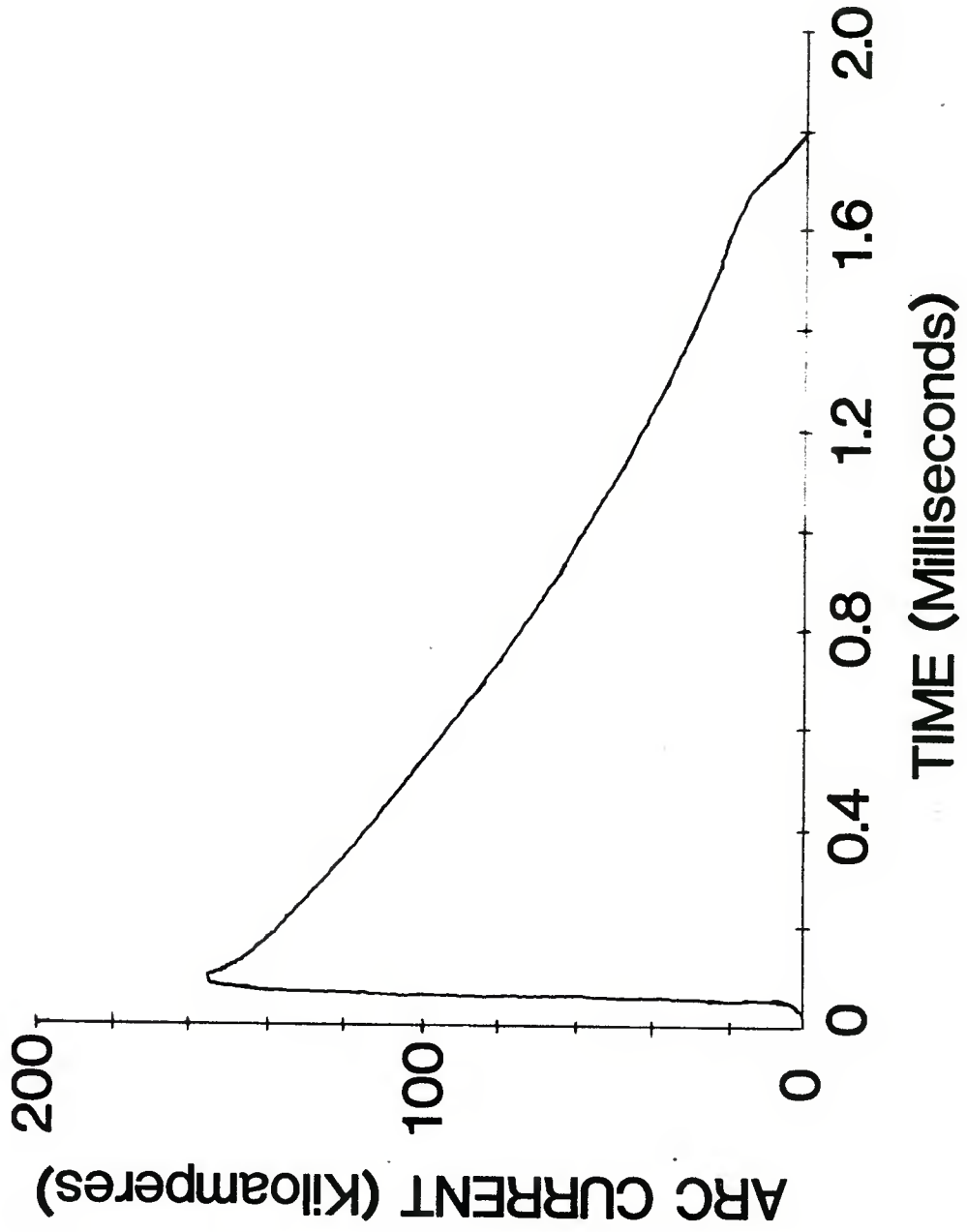


Figure 10. Arc Current Versus Time

VI. CONCLUSION

We have developed a laboratory rail gun of the arc armature type which provides an easily used test bed for diagnosis of driven plasma arc armatures. The mechanical design is straightforward: a pair of one metre by 2.5 cm copper busbar rails separated by insulating side rails forming a 12.7 mm square-bore gun. The magnetic forces developed in the rail gun are capable of accelerating a 2.8 gram polycarbonate projectile to a velocity of 1200 metres per second in the length of the gun. The time duration of the current pulse that powers the acceleration is 1.8 milliseconds; its amplitude is 150,000 amps at its maximum; and it decays exponentially with a time constant of about 760 microseconds.

In the power source we have developed, the storage capacitor bank transfers its energy to the magnetic field of an intermediate storage inductance. In turn, the rail gun draws energy from this magnetic field as the projectile is accelerated by the Lorentz force on the arc armature.

We have characterized the arc armature in general terms by continuous measurement of current and voltage during the accelerating event. The arc exerts a maximum of 200 atm of pressure on the projectile and conducts currents up to 150,000 A from rail to rail. The arc also appears to make good electrical contact with the rails even at velocities in excess of 1 km/s. The voltage drop in the arc is between 100 and 200 V and is not strongly dependent on the arc current.

The barrel is designed to be easily disassembled and reassembled. By replacing the initiator and projectile and installing a new exploding wire, one may fire many times with only minor refurbishing of the copper rails and without replacement of major components. The insulating plastic side rails are easily drilled for embedding diagnostic devices such as fiber optics and magnetic field sensing loops. Such stationary devices can provide data whose time variation may be converted to spatial variation with accurate knowledge of the fly-by velocity. Currently, several such embedded devices are being used to investigate specific dynamic parameters of driven plasma arc armatures. Probes include light emission detectors and magnetic field measurement devices which can give detailed information for validation of untested arc dynamic theories.

ACKNOWLEDGEMENTS

The authors wish to acknowledge D. Eccleshall for suggesting the pulse forming network for the power circuit and his analysis of the gun-storage inductor interactions. We are indebted to M. Marquez-Reines and R. Coates for their assistance in the experimental work, detector fabrication and data acquisition.

REFERENCES

1. R.S. Hawke, A.L. Brooks, F.J. Deadrick, J.K. Scudder, C.M. Fowler, R.S. Caird and D.R. Peterson, "Results of Rail Gun Experiments Powered by Magnetic Flux Compression Generators," *IEEE Trans. on Magnetics*, Mag. 18, 82 (1982).
2. A.L.O. Fauchon-Villeplee, Electric Cannons, 1921. Also see US Patent Nos. 1,370,200 patented March 1, 1921, 1,421,435 patented July 4, 1922, and 1,422,427, patented July 11, 1922.
3. Summary of work done by J. Hänsler, "Electric Gun and Power Source," Armour Research Foundation Report No. 3 on Project No. 15-391-E (1946).
4. D.E. Brast and D.R. Sawle, "Study of Rail-Type MHD Hypervelocity Projectile Accelerator," *Proceedings of the Seventh Hypervelocity Impact Symposium*, Vol 1, 187 (1964).
5. J.P. Barber, "The Acceleration of Macroparticles and a Hypervelocity Electromagnetic Accelerator," Ph.D. Thesis, Australian National University, Canberra, Australia (1972).
6. S.C. Rashleigh and R.A. Marshall, "Electromagnetic Acceleration of Macroparticles to High Velocities," *J. Appl. Phys.* 49, 2540 (1978).
7. N.H. Wrobel and M.J. Newman, "System Study to Determine Future K E Propulsion Conventional/Electric Gun or Rocket/Ramjet?", *Proc. 6th Int. Symp. on Ballistics* (1981), p. 546.
8. J.D. Powell and J.H. Batteh, "Plasma Dynamics of an Arc-Driven, Electromagnetic, Projectile Accelerator," *J. Appl. Phys.* 52, 2717 (1980); "Two-Dimensional Plasma Model for Arc-Driven Rail Gun," *J. Appl. Phys.* (in press).
9. F.W. Grover, Inductance Calculations, D. Van Nostrand Co., Inc., NYC, 1946.
10. Frederick E. Terman, Radio Engineers Handbook, 1st Ed., McGraw-Hill, NYC (1945), p. 53.
11. K. Fansler, "On Balloting of Projectiles," ARBRL-MR-02831, April 1978 (AD A055707).
12. Adolf J. Schwab, High Voltage Measurement Techniques, MIT Press, Cambridge, MA (1972), p. 180-186.
13. D.G. Pellinen, M.S. Di Capua, S.E. Sampayan, H. Gerbracht and M. Wang, "Rogowskii Coil for Measuring Fast, High Level Pulsed Currents," *Rev. Sci. Instrum.* 51, 1535 (1980).
14. I.R. McNab, et al., "DC Electromagnetic Launcher Development: Phase I," Contractor Report ARLCD-CR-80009, May 1980, AD-E400 419, p. A-47.

APPENDIX A

Exploding Wire Opening Switch Calculations

APPENDIX A

EXPLODING WIRE OPENING SWITCH CALCULATIONS

In this appendix the computer program used to select the proper opening switch exploding wire is described. It models an RLC circuit containing a single resistive element whose resistance is determined by the past history of current conduction and the element's physical characteristics. The model conserves energy and voltage while stepping through time.

Of pivotal importance to the model is the resistance of the wire. Its evolution is modeled in two distinct stages. Up to the vaporization point, only the wire's temperature increase raises the resistance; when the temperature reaches the vaporization point, temperature is considered constant while mass is boiled off the surface. Now the decreasing conducting cross section causes the resistance rise.

During the first stage, the resistance is updated in the following way:

(1) An incremental increase of the wire's thermal energy, $I^2 R \Delta t$, is used to compute an increase in the wire's temperature. (2) The resistance is determined by an empirical formulation for the thermal coefficient of resistivity. The solid-liquid phase change is ignored. During the second stage, after the temperature of the wire reaches copper's boiling point, further increments of energy vaporize and remove mass from the wire, thereby decreasing its radius and increasing its resistance. The mass decrease equals the ratio of thermal energy dissipated in the wire by the circuit to the latent heat of vaporization. During the third stage, the voltage drop across the wire is set arbitrarily to 200 volts to signal complete vaporization of the wire. Though somewhat simplistic, the calculation has been quite accurate over a wide range of capacitance values in predicting the wire gauge needed for switching LC circuits. Basic assumptions ignore:

- o Heat loss by the wire
- o The solid-liquid phase change
- o Resistance of all circuit components (except the wire)
- o Pressure dependence of vaporization
- o Skin depth effects
- o Length (position) dependence of radius as wire vaporizes.

The program models by an empirical form:

- o Temperature dependence of resistance
- o Mass dependence of the resistance
- o The temperature dependence of the specific heat.

Figure A1 is a graph of current as a function of time. The dots are the values calculated by the program with input parameters set to experimental conditions. The x's are data points for an actual measurement of the capacitor discharge current as a function of time. Also shown as a dashed line in Figure A1 is the current curve for a lossless LC circuit. The time predicted for the complete vaporization of the wire is indicated. The steepest portion of the data curve and the point at which the program indicates the wire is completely vaporized are nearly coincident.

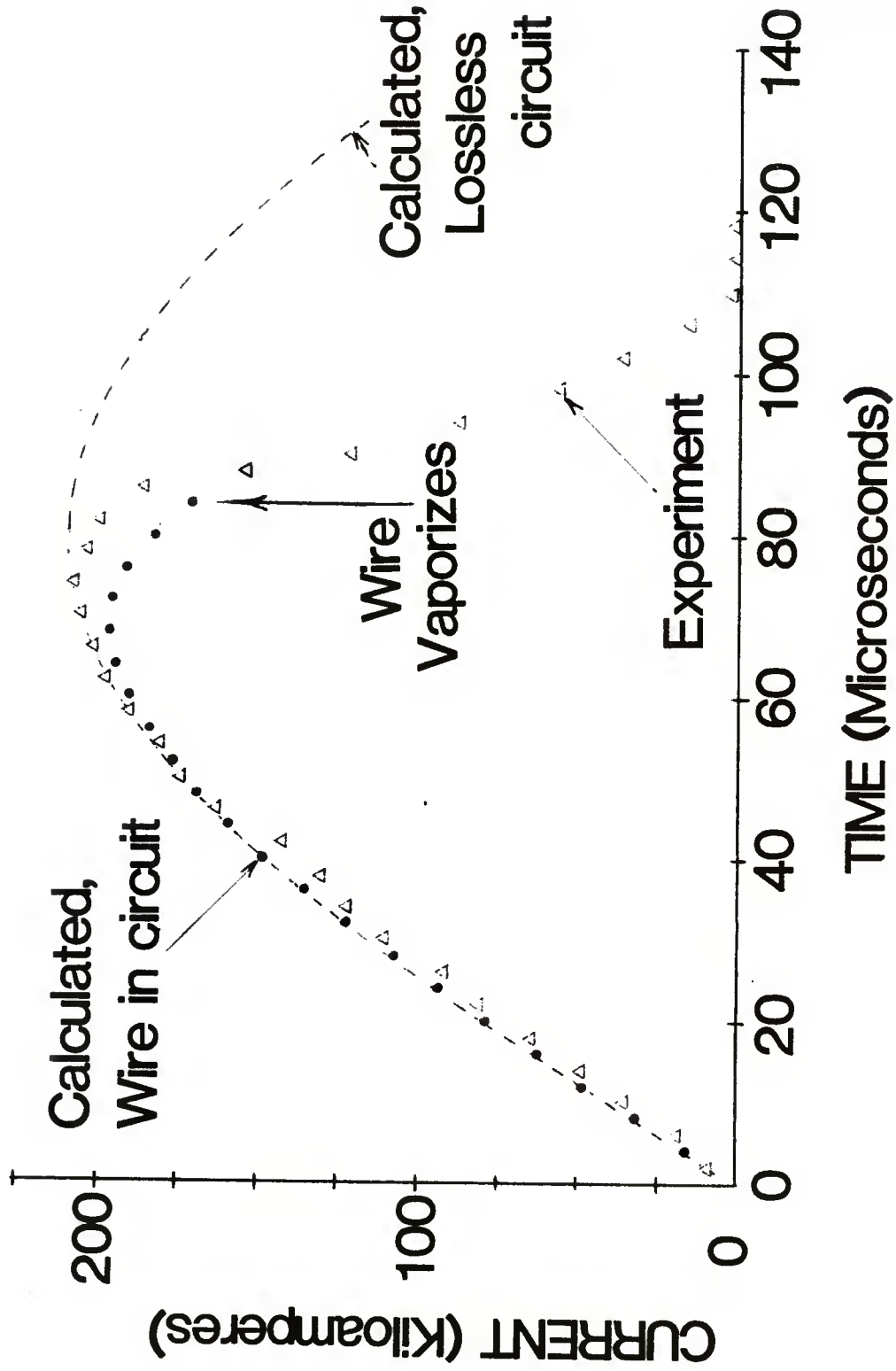


Figure A1. Calculated Capacitor Current

The program also provides information about the voltage remaining on the capacitors and the energy stored in the inductor's magnetic field at the time when the wire has vaporized. Several runs for different wire gauges were done with 1200 μ F and 9000 V initial conditions. The results are summarized in Figure A2. The top curve shows the time required to vaporize a wire as a function of wire gauge. The center curve shows the voltage remaining on the capacitor bank and the bottom curve shows the energy stored in the inductor's magnetic field as the wire completes vaporization. It is important to store as much energy as possible in the inductor but also the capacitor voltage must be quite low to prevent the opening switch from reclosing. We have chosen to use 12 gauge wire because of the complete discharge of the capacitor bank. One attempt was made using 13 gauge wire but the opening switch reclosed a few microseconds after opening due to the excess voltage remaining on the capacitor bank. If the opening switch recloses, the energy stored in the inductor's field rings back into the capacitor bank and insufficient energy is available to drive the rail gun.

A listing of the computer program and the subroutine, RESIST, are on the pages following.

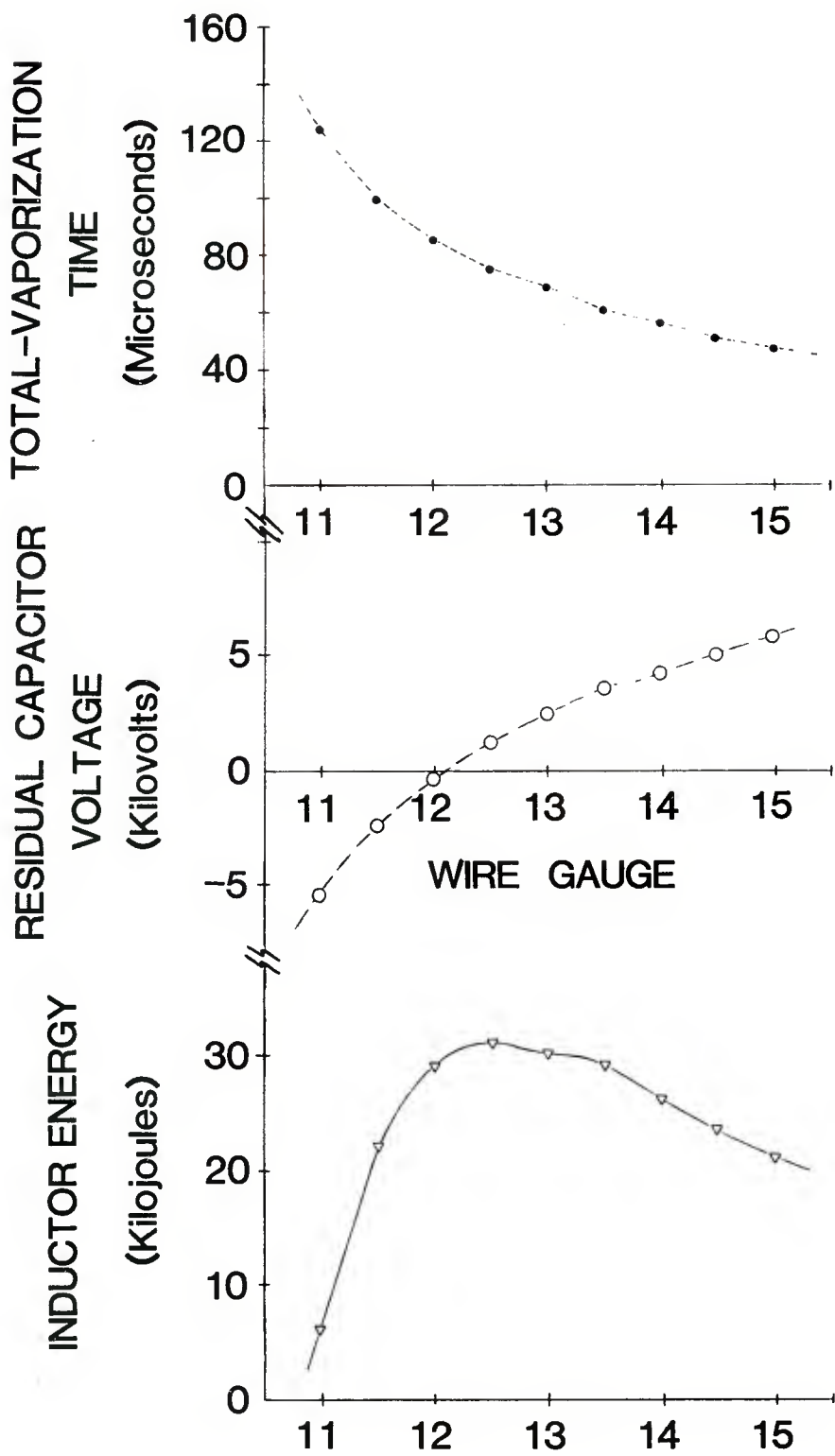


Figure A2. Exploding Wire Performance Versus Wire Gauge

```

C
C   THIS FORTRAN PROGRAM CALCULATES THE TIME
C   REQUIRED TO COMPLETELY VAPORIZE AN EXPLODING
C   WIRE OPENING SWITCH IN AN L-C CIRCUIT
C
C   IMPLICIT REAL (I,L,M)
C
C   INPUT THE INITIAL PARAMETERS
C       1. CAP = CIRCUIT CAPACITANCE (FARADS)
C       2. VCAP = INITIAL CAPACITOR VOLTAGE
C       3. L = INDUCTANCE (HENRIES)
C       4. GA = WIRE GAUGE
C       5. WL = WIRE LENGTH (INCHES)
C       6. T = WIRE TEMPERATURE (KELVIN)
C
C   VCAP = INITIAL CAPACITOR VOLTAGE
99  WRITE (6,100)
    READ (6,101)CAP
    WRITE (6,102)
    READ (6,103)VCAP
    WRITE (6,104)
    READ (6,105)L
    WRITE (6,106)
    READ (6,107)GA
    WRITE (6,108)
    READ (6,109)WL
    WRITE(6,111)
    READ(6,103)T
C
C   INITIALIZE VALUES
C
C   N=0
C   TIME=0.0
C   DT=1.E-08
C   I=0.0
C   VW=0.0
C
C   CALCULATE CAPACITOR CHARGE, MASS OF WIRE, AND
C   INITIAL WIRE RESISTANCE
C
C   Q=CAP*VCAP
C   M=WL*12.23*EXP(GA*-.2318)
C   ROLD=WL*.8344E-05*EXP(GA*.2319)
C   ROLD=ROLD*(40.+T)/338.
C   ET=0.0
C
C   BEGIN ENERGY FLOW --- TIME LOOP
C
C   VCL=VCAP-VW
C   N=N+1
C
C   UPDATE DI/DT, CURRENT, CHARGE, ENERGY,
C   TIME, AND WIRE RESISTANCE AND MASS
C
C   DIDT=VCL/L

```

```

I=I+DI*DT
Q=Q-I*DT
VCAP=Q/CAP
E=I*I*ROLD*DT
ET=E+ET
CALL RESIST (T,I,E,M,ROLD)
TIME=TIME+DT
VW=I*ROLD
VCL=VCAP-VW

C
C   PRINT OUT EVERY FIVE HUNDREDTH CALCULATION
C
IF (N/500.NE.(N+499)/500) GO TO 5
6   WRITE (6,110)TIME,VCAP,VW,VCL,I,ET,T
110  FORMAT (' ',F9.7,6(2X,F9.0))
IF (TIME.GT.2E-04)GO TO 99
100  FORMAT (' INPUT CAPACITANCE ')
101  FORMAT (E8.2)
102  FORMAT (' INPUT VOLTAGE ON CAPACITORS')
103  FORMAT (F7.3)
104  FORMAT (' INPUT COIL INDUCTANCE ')
105  FORMAT (E8.2)
106  FORMAT (' WIRE GAGE')
107  FORMAT (F4.2)
108  FORMAT (' INPUT LENGTH OF WIRE ')
109  FORMAT (F4.2)
111  FORMAT(' TEMP OF WIRE(K)?')
GO TO 5
END

```

```

C
C THIS SUBROUTINE UPDATES THE RESISTANCE OF
C AN EXPLODING WIRE
C
      SUBROUTINE RESIST (T,I,E,M,ROLD)
      IMPLICIT REAL (I,M)
      A=3.0E-06
      IF (M.LE.0) GO TO 40
      IF (T.GT.2840.)GO TO 50
C
C IF THE WIRE TEMPERATURE IS BELOW THE BOILING
C POINT, INCREASE THE TEMPERATURE AND CALCULATE
C A NEW RESISTANCE
C
      TN=T+E/((T*.00009+.362)*M)
      ROLD=ROLD*(A*TN*TN+.6)/(A*T*T+.6)
      T=TN
      GO TO 99
C
C IF THE WIRE IS COMPLETELY VAPORIZED, SET
C THE VOLTAGE DROP TO 200 VOLTS
C
40      X=200.0/FLOAT(I)
      ROLD=ABS(X)
      M=-1.00
      GO TO 99
C
C IF THE WIRE TEMPERATURE IS ABOVE THE BOILING
C POINT, DECREASE THE MASS AND CALCULATE A NEW
C RESISTANCE
C
50      DM=E/4794.5
      A=M-DM
      IF (A.LE.0.0) A=1.0
      ROLD=ROLD*M/A
      M=M-DM
99      RETURN
      END

```

APPENDIX B

Rail Gun Performance

APPENDIX B

RAIL GUN PERFORMANCE

In the time span between the initial drafting of this report through the final editing the rail gun has been used on a regular basis for diagnostic studies of driven plasma arcs. In the course of this work we have recorded the initial stored energy and the projectile velocity for each of the firings. These results are presented in Table B.1 together with the projectile masses and kinetic energies. The rather large variance in the last column of Table B.1 is partially due to the extreme sensitivity of the circuit performance to the switching and partly due to the experimental conditions which required slight changes for nearly every shot. No attempt has been made to systematically study the reproducibility of the power circuit and rail gun efficiency. Instead, the emphasis is on the study of the arc itself. For these purposes the performance of the system is quite satisfactory.

TABLE B.1 - Summary of Rail Gun Performance

<u>Initial Capacitor (kV)</u>	<u>Initial Energy (kJ)</u>	<u>Projectile Mass (g)</u>	<u>Velocity m/s</u>	<u>Kinetic Energy of Projectile kJ</u>
9.0	48.6	2.83	1370	2.7
9.1	48.6	2.83	1250	2.2
9.1	49.7	2.55	1190	1.8
9.4	53.0	2.53	1440	2.6
9.7	56.4	2.52	1610	3.3
9.5	54.1	2.55	940	1.1
9.5	54.1	2.56	1210	1.9
9.5	54.1	2.57	1180	1.8
9.7	56.4	2.55	1370	2.4
9.6	55.3	2.55	1220	1.9
9.6	55.3	2.55	1480	2.8
9.7	56.4	2.55	1090	1.5
AVERAGE 53.5				2.17

DISTRIBUTION LIST

<u>No. of</u> <u>Copies</u>	<u>Organization</u>	<u>No. of</u> <u>Copies</u>	<u>Organization</u>
12	Administrator Defense Technical Info Center ATTN: DTIC DDA Cameron Station Alexandria, VA 22314	1	Commander US Army Materiel Development & Readiness Command ATTN: DRCLDC, Mr. Langworthy 5001 Eisenhower Avenue Alexandria, VA 22333
1	Office Under Secretary of Defense Res & Engr ATTN: Mr. Ray Thorkildsen Room 3D1089, Pentagon Washington, DC 20301	1	Commander US Army Armament Research & Develop- ment Command ATTN: DRDAR-TDC Dover, NJ 07801
1	Deputy Under Secretary of Defense Res & Engr ATTN: Dr. Arden L. Bement Room 3E114, Pentagon Washington, DC 20301	5	Commander US Army Armament Research & Develop- ment Command ATTN: DRDAR-LCA, Mr. J.A. Bennett DRDAR-LCA, Dr. W.R. Snow DRDAR-LCA, Dr. T. Gora DRDAR-LCA, Dr. P. Kemmy DRDAR-LCA, Mr. C. Dunham Dover, NJ 07801
4	Director Defense Advanced Research Projects Agency ATTN: Dr. Joseph Mangano Dr. Gordon P. Sigman Dr. Raymond P. Gogolewski Dr. Harry Fair 1400 Wilson Blvd Arlington, VA 22209	3	Commander US Army Armament Research & Develop- ment Command ATTN: DRDAR-TSS DRDAR-SCA, W.R. Goldstein Dover, NJ 07801
1	Office of Assistant Secretary of the Army ATTN: RDA, Dr. Joseph Yang Room 2E672, Pentagon Washington, DC 20310	1	Commander US Army Armament Materiel Readiness Command ATTN: DRSAR-LEP-L Rock Island, IL 61299
1	HQDA (DAMA-ARZ-A, Dr. Marvin Lasser) Washington, DC 20310	1	Director US Army ARRADCOM Benet Weapons Laboratory ATTN: DRDAR-LCB-TL Watervliet, NY 12189
1	Commander US Army Materiel Development & Readiness Command ATTN: DRCMDM-ST 5001 Eisenhower Avenue Alexandria, VA 22333	1	Commander US Army Aviation Research & Develop- ment Command ATTN: DRDAV-E 4300 Goodfellow Blvd. St. Louis, MO 63120

DISTRIBUTION LIST

<u>No. of</u> <u>Copies</u>	<u>Organization</u>	<u>No. of</u> <u>Copies</u>	<u>Organization</u>
1	Director US Army Air Mobility Research & Development Laboratory Ames Research Center Moffett Field, CA 94035	2	Commander Naval Air Systems Command ATTN: Dr. R.J. Wasneski, Code 350F John A. Reif, Air 350B Washington, DC 20360
1	Commander US Army Communications Research & Development Command ATTN: DRSEL-ATDD Ft. Monmouth, NJ 07703	1	Commander US Naval Research Laboratory ATTN: Dick Ford, Code 4774 Washington, DC 20375
1	Commander US Army Electronics R&D Command Technical Support Activity ATTN: DELSD-L Ft. Monmouth, NJ 07703	4	Commander Naval Surface Weapons Center ATTN: Henry B. Odom, Code F-12 Dr. M. Franklin Rose, Code F-04 P.T. Adams & D.L. Brunson, Code G-35 Dahlgren, VA 22448
2	Commander US Army Missile Command ATTN: DRSMI-R DRSMI-YDL Redstone Arsenal, AL 35898	1	HQ AFSC/SDOA/XRB ATTN: CPT Dennis Kirlin Andrews AF Base, MD 20334
1	Commander US Army Tank Automotive Command ATTN: DRSTA-TSL Warren, MI 48090	1	AFWL/NTYP (John Generosa) Kirtland AFB, NM 87117
1	Director US Army TRADOC Systems Analysis Activity ATTN: ATAA-SL White Sands Missile Range NM 88002	1	AFAPL (Dr. Charles E. Oberly) Wright-Patterson AFB, OH 45433
2	Commander US Army Research Office ATTN: Dr. Fred Schmiedeshoff Dr. M. Ciftan PO Box 12211 Research Triangle Park, NC 27709	2	AFATL/DLDB (Lanny Burdge) (Bill Lucas) Eglin AF Base, FL 32542
		1	AFATL (Richard Walley) Eglin AF Base, FL 32542
		1	AFWL (Dr. William L. Baker) Kirtland AFB, NM 87117
2	Commandant US Army Infantry School ATTN: ATSH-CD-CSO-OR Fort Benning, GA 31905		

DISTRIBUTION LIST

<u>No. of</u> <u>Copies</u>	<u>Organization</u>	<u>No. of</u> <u>Copies</u>	<u>Organization</u>
1	AFWAL/POOS-2 (CPT Gerald D. Clark) Wright-Patterson AFB, OH 45433	2	GT Devices ATTN: Dr. Shyke Goldstein Dr. Derek Tidman 5705A General Washington Drive Alexandria, VA 22312
1	Director Brookhaven National Laboratory ATTN: Dr. James R. Powell Bldg. 129 Upton, NY 11973	2	R&D Associates ATTN: Mr. Ronald Cunningham Dr. Peter Turchi PO Box 9695 4640 Admiralty Way Marina Del Rey, CA 90291
1	Director Lawrence Livermore National Lab P. O. Box 808 ATTN: R.S. Hawke Livermore, CA 94550	1	Science Applications, Inc. ATTN: Dr. Jad H. Batteh 1503 Johnsons Ferry RD Suite 100 Marietta, GA 30062
3	Director Los Alamos National Scientific Laboratory ATTN: Dr. Clarence M. Fowler, MS970 Dr. Denis R. Peterson, MS985 Dr. Jerald V. Parker, MSE525 P.O. Box 1663 Los Alamos, NM 87545	1	Science Applications, Inc. Corporate Headquarters ATTN: Dr. Frank Chilton 1200 Prospect Street La Jolla, CA 92038
4	NASA-LeRC MS 501-7 ATTN: Bill Kerslake Frank Terdan Mike Brasher Lynette Zana 2100 Brook Park RD Cleveland, OH 44135	1	Vought Corporation Advanced Technology Center ATTN: Dr. Michael M. Tower PO Box 226144 Dallas, TX 75266
2	Sandia Laboratories ATTN: M. Cowan T. J. Burgess Albuquerque, NM 87115	2	Westinghouse Research & Development Laboratory ATTN: Dr. Ian R. McNab Dr. D.W. Deis 1310 Beulah RD Pittsburgh, PA 15253
2	IAP Research, Inc. ATTN: Dr. John P. Barber Mr. D.P. Bauer 7546 McEwen RD Dayton, OH 45459	1	Georgia Institute of Technology ATTN: Prof. Alan V. Larson Atlanta, GA 30332
1	Battelle Pacific Northwest Labs P.O. Box 999 Richland, WA 99352	2	Massachusetts Institute of Technology Francis Bitter National Magnet Laboratory ATTN: Dr. Henry H. Kolm, Mr. Peter Mongeau NW-14-3102 170 Albany Street Cambridge, MA 02139

DISTRIBUTION LIST

<u>No. of</u> <u>Copies</u>	<u>Organization</u>
1	Tuskegee Institute ATTN: Dr. Pradosh Ray Tuskegee Institute, AL 36088
2	University of Texas Center of Electromechanics ATTN: Dr. Richard A. Marshall Mr. William F. Weldon 167 Taylor Hall Austin, TX 78712

Aberdeen Proving Ground

Dir, USAMSAA
ATTN: DRXSJ-D
DRXSJ-MP, H. Cohen
Cdr, USATECOM
ATTN: DRSTE-TO-F
Dir, USACSL, Bldg E3516
ATTN: .DRDAR-CLB-PA
DRDAR-CLN
DRDAR-CLJ-L

USER EVALUATION OF REPORT

Please take a few minutes to answer the questions below; tear out this sheet, fold as indicated, staple or tape closed, and place in the mail. Your comments will provide us with information for improving future reports.

1. BRL Report Number _____

2. Does this report satisfy a need? (Comment on purpose, related project, or other area of interest for which report will be used.)

3. How, specifically, is the report being used? (Information source, design data or procedure, management procedure, source of ideas, etc.) _____

4. Has the information in this report led to any quantitative savings as far as man-hours/contract dollars saved, operating costs avoided, efficiencies achieved, etc.? If so, please elaborate.

5. General Comments (Indicate what you think should be changed to make this report and future reports of this type more responsive to your needs, more usable, improve readability, etc.) _____

6. If you would like to be contacted by the personnel who prepared this report to raise specific questions or discuss the topic, please fill in the following information.

Name: _____

Telephone Number: _____

Organization Address: _____

